2930 *Chem. Mater.* **2010,** *22,* 2930–2936
DOI:10.1021/cm100237m

CHEMISTRY OF MATERIALS
Article

Measuring the Extent of Phase Separation in Poly-3-Hexylthiophene/Phenyl-C_{61}-Butyric Acid Methyl Ester Photovoltaic Blends with ^{1}H Spin Diffusion NMR Spectroscopy

Ryan C. Nieuwendaal, Chad R. Snyder, R. Joseph Kline, Eric K. Lin, David L. VanderHart,* and Dean M. DeLongchamp*

Polymers Division, National Institute of Standards and Technology, 100 Bureau Drive, Gaithersburg, Maryland 20899-1000

Received January 25, 2010. Revised Manuscript Received March 9, 2010

We demonstrate that ^{1}H spin diffusion NMR is a valuable method to estimate the domain size distribution in bulk heterojunction (BHJ) active layers composed of poly-3-hexylthiophene (P3HT) and phenyl-C_{61}-butyric acid methyl ester (PCBM). Bulk samples were annealed at several temperatures, and a distribution of domain sizes was observed that ranged over hundreds of nanometers. Unannealed samples exhibited a large amount of PCBM in small domains (1 to 5 nm) and smaller amounts in moderate (tens of nm) and large (> 100 nm) domains. Annealing the samples at 100 °C had no effect on the morphology as evidenced from ^{1}H spin diffusion NMR, grazing-incidence diffraction, and calorimetry, but phase separation was observed after annealing at 150 °C. Even with this higher temperature processing, the ^{1}H NMR showed conclusively that phase separation remained incomplete; this finding was confirmed with photoluminescence quenching measurements.

Introduction

Research in organic photovoltaics is establishing a promising low-cost solar energy technology that could enable manufacturing by solution-based printing or coating. One of the most promising OPV device types relies on a bulk heterojunction (BHJ), which is a thin film containing a blend of photon-absorbing and electron-accepting semiconductors. The BHJ design attempts to reconcile the short exciton diffusion length in typical absorbers (6 to 10 nm)[1−5] with the need for an optical path length of at least ≈80 nm for sunlight absorption.[6] The ideal BHJ morphology would consist of pure absorber and acceptor phases, with the absorber domains having a dimension smaller than the exciton diffusion length, and co-continuous networks of both phases leading to the appropriate electrodes. While BHJ devices have demonstrated high power conversion efficiencies ($\eta \approx 7\%$),[7] establishing correlations between device performance and molecular structure has been extremely challenging. The device-relevant length scales in BHJs are nanometers, and resolving such finely mixed phases with conventional methods such as microscopy or scattering is difficult because both materials are aromatic hydrocarbons. Despite these analytical challenges, understanding the impacts of phase distribution, purity, and domain size on device performance remains a critical need in efforts to design better OPV materials and fabrication processes.

Solid-state nuclear magnetic resonance (NMR) spectroscopy is a powerful method to measure the nanoscale structure of polymer blends. In fact, ^{1}H−^{13}C heteronuclear correlation NMR measurements were recently reported[8] on a widely studied BHJ, the blend of poly-3-hexylthiophene (P3HT), Figure 1a, and phenyl-C_{61}-butyric acid methyl ester (PCBM), Figure 1b, in an effort to investigate the interfacial structure. However, only one mixing time was reported, which was insufficient to determine a domain size. In this article, we also focus on the P3HT/PCBM system, and demonstrate that ^{1}H spin diffusion NMR can measure the phase behavior and domain sizes of BHJs, because of its sensitivity to intermolecular correlations over nanometer length scales and its unambiguous chemical contrast, just as it has done on many polymer blend systems previously.[9−14]

*To whom correspondence should be addressed. E-mail: vdhart@nist.gov (D.L.V), deand@nist.gov (D.M.D.).

(1) Halls, J. J. M.; Pichler, K.; Friend, R. H.; Moratti, S. C.; Holmes, A. B. *Appl. Phys. Lett.* **1996**, *22*, 3120–3122.
(2) Haugeneder, A.; Neges, M.; Kallinger, C.; Spirkl, W.; Lemmer, U.; Feldman, J.; Scherf, U.; Harth, E.; Gugel, A.; Mullen, K. *Phys. Rev. B* **1999**, *59*, 15346–15351.
(3) Theander, M.; Yartsev, A.; Zigmatas, D.; Sundstrom, V.; Mammo, W.; Andersson, M. R.; Inganas, O. *Phys. Rev. B.* **2000**, *61*, 12957–12963.
(4) Stubinger, T.; Brutting., W. *J. Appl. Phys.* **2001**, *90*, 3632–3641.
(5) Markov, D. E.; Amsterdam, E.; Blom, P. W. M.; Sieval, A. B.; Hummelen, J. C. *J. Phys. Chem. A.* **2005**, *109*, 5266–5274.
(6) Dennler, G.; Scharber, M. C.; Brabec, C. J. *Adv. Mater.* **2009**, *21*, 1323–1338 and references therein.
(7) Chen, H. S.; Hou, J.; Zhang, S.; Liang, Y.; Yang, G.; Yang, Y.; Yu, L.; Wu, Y.; Li, G. *Nat. Photon.* **2009**, *3*, 649–653.
(8) Yang, C.; Hu, J. G.; Heeger, A. J. *J. Am. Chem. Soc.* **2006**, *128*(36), 12007–12013.
(9) VanderHart, D. L.; Prabhu, V. M.; De Silva, A.; Felix, N. M.; Ober, C. K. *J. Mater. Chem.* **2009**, *19*, 2683–2694.
(10) VanderHart, D. L.; Prabhu, V. M.; Lin, E. K. *Chem. Mater.* **2004**, *16*, 3074–3084.
(11) VanderHart, D. L.; Feng, Y.; Han, C. C.; Weiss, R. A. *Macromolecules* **2000**, *33*, 2206–2227.
(12) Campbell, G. C.; VanderHart, D. L. *J. Magn. Reson.* **1992**, *96*, 69.
(13) VanderHart, D. L.; Campbell, G. C.; Briber, R. M. *Macromolecules* **1992**, *25*, 4734–4743.
(14) VanderHart, D. L. *Macromolecules* **1994**, *27*, 2837–2845.

Published on Web 04/05/2010

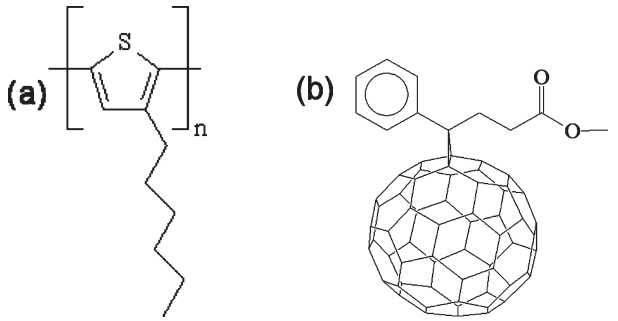

Figure 1. Chemical structures of poly-3-hexylthiophene (a) and phenyl-C_{61}-butyric acid methyl ester (b).

We note that a key advantage of ^{1}H NMR is its excellent sensitivity, which potentially allows for extensions to technologically relevant samples such as thin films.

When cast from the same solution, P3HT and PCBM form a BHJ film that can deliver up to ≈5% power conversion efficiency.[6] The characteristics of the P3HT/PCBM blend differ depending on the solvent chosen[6,15] and how the films are heated after casting.[6,15−20] Heat treatment is generally thought to increase efficiency, and heating to temperatures of 140 to 160 °C is common in optimized fabrication procedures.[6,15−20] One consequence of heat treatment, however, can be the formation of needle-like PCBM crystallites that are typically associated with lower efficiency.[21,22] Here, we use ^{1}H solid-state NMR and complementary techniques to identify the effect of heat treatment on the blend structure. The films are relatively thick (50 to 100 μm) blends of 50/50 P3HT/PCBM by mass, cast from chlorobenzene. Thin films cast from this solvent typically require thermal annealing for improved device performance.

Experimental Section

Poly-3-hexylthiophene (P3HT) was purchased from Plextronics (Plexcore 2100, M_n = 55000 kDa, $M_w/M_n \approx 2.0$) and phenyl-C_{61}-butyric acid methyl ester (PCBM) from NanoC; they were used as is. The head-to-tail regioregularity of P3HT was found to be greater than 98% via solution-state ^{1}H NMR (data not included). Thirty mg/mL solutions (15 mg P3HT + 15 mg PCBM) were prepared in chlorobenzene (99%, Aldrich) in an inert atmosphere and cast onto Teflon. These relatively thick films (50 to 100 μm) were used for grazing-incidence X-ray diffraction, differential scanning calorimetry, photoluminescence (PL), and solid-state NMR measurements.

PL measurements were taken on a custom-built setup using a HeCd laser (λ = 442 nm, ≈ 5 mW), charged coupled device (CCD) camera, and UV−vis spectrometer (Ocean Optics, USB 2000). The laser beam was focused using a fused silica triplet lens to a laser spot of ≈200 μm in diameter. The PL was collected through an infinity corrected objective (N.A. = 0.60, λ > 340 nm). Scattered laser light was removed using an optical density (325 nm) laser block filter. Focusing and imaging was done using a fused silica tube lens, which fed into the CCD camera. Once focused, a mirror was used to direct the PL onto the face of a UV-transmitting fused silica fiber, which fed into the UV−vis spectrometer for spectral acquisition. Spectra were calibrated using a tungsten halogen lamp, and an instrumental response profile was generated in the spectral range of 350 to 1100 nm that was used to correct all spectra. A spectrum was collected every second, and averaged over every 5 scans.

Solid-state ^{1}H NMR experiments were performed at 300 MHz on a Bruker DMX300 spectrometer. Combined Rotation And Multiple Pulse Spectroscopy (CRAMPS)[23] experiments were performed using the MREV8 pulse sequence[24] characterized by eight 1.51 μs $\pi/2$ pulses and a cycle time of 39.6 μs. Each sample (≈10 mg) was placed into a 5-mm Si_3N_4 rotor and spun at 2525 ± 5 Hz. Other typical parameters were as follows: 300.13 MHz carrier frequency, 4900 Hz offset, 400 MREV-8 cycles (and FID points), 16 dB receiver gain, 0.49 scaling factor. For spin diffusion experiments, a fixed, measurable polarization gradient was established between the protons of P3HT and PCBM such that the total spin diffusion integral was zero. This zero-integral preparation was established via selection of the proper number of MREV8 cycles (ten over exactly one rotor period) and frequency offset (4900 ± 50 Hz). Longitudinal relaxation effects on $\Delta M(t_m)$ were eliminated by alternating between $+z$ and $-z$ initial polarizations (with corresponding addition and subtraction of alternating signals) and by subsequently multiplying by the appropriate correction factor (see below and Supporting Information). The initial polarization of PCBM, $M_{initial}^{PCBM}/M_0^{PCBM}$, was −(0.40 ± 0.02); the initial polarization of P3HT, $M_{initial}^{P3HT}/M_0^{P3HT}$, was +(0.08 ± 0.02). The uncertainty of initial polarizations is due to subtle changes in the scaling factor and is accounted for in the error bars included in Figure 7. We only show ^{1}H spin diffusion spectra for mixing times ≥2 ms because unavoidable, early time intramolecular spin exchange results in ambiguous spectral interpretation at these shorter times, similar to what has been observed in other polymer blend systems.[12,13,25]

Results

Grazing-Incidence X-ray Diffraction. Grazing-incidence X-ray diffraction (GIXD) patterns shown in Figure 2 reveal thermally induced PCBM crystallization. Before annealing, the GIXD pattern is essentially the crystalline P3HT pattern[26] (Figure 2a) with the addition of a broad, diffuse ring at q = 1.4 Å^{-1}, indicative of small PCBM crystals. This pattern does not change upon annealing at 100 °C for 1 h (Figure 2b). However, upon annealing at 150 °C for 1 h (Figure 2c), a sharp ring appears in the GIXD pattern:

(15) Kim, Y.; Choulis, S. A.; Nelson, J.; Bradley, D. D. C.; Cook, S.; Durrant, J. R. *Appl. Phys. Lett*. **2005**, *86*, 063502.
(16) Kim, Y.; Choulis, S. A.; Nelson, J.; Bradley, D. D. C.; Cook, S.; Durrant, J. R. *J. Mater. Sci*. **2005**, *40*, 1371–1376.
(17) Li, G.; Shrotriya, V.; Yao, Y.; Yang, Y. *J. Appl. Phys*. **2005**, *94*, 043704.
(18) Yang, X.; Loos, J.; Veenstra, S. C.; Verhees, J. H.; Wienk, M. M.; Kroon, J. M.; Michels, M. A. J.; Janssen, R. A. J. *Nano Lett*. **2005**, *5*, 579.
(19) Reyes-Reyes, M.; Kim, K.; Carroll, D. L. *Appl. Phys. Lett*. **2005**, *87*, 083506.
(20) Kim, Y.; Cook, S.; Tuladhar, S. M.; Choulis, S. A.; Nelson, J.; Durrant, J. R.; Bradley, D. D. C.; Giles, M.; McCulloch, I.; Ha, C. S.; Ree, M. *Nat. Mater*. **2006**, *5*, 197.
(21) Swinnen, A.; Haeldermans, I.; vande Ven, M.; D'Haen, J.; Vanhoyland, G.; Aresu, S.; D'Olieslaeger, M.; Manca, J. *Adv. Funct. Mater*. **2006**, *16*, 760–765.
(22) Savenije, T. J.; Kroeze, J. E.; Yang, X.; Loos, J. *Adv. Funct. Mater*. **2005**, *15*, 1260–1266.
(23) Ryan, L. M.; Taylor, R. E.; Paff, A. J.; Gerstein, B. C. *J. Chem. Phys*. **1980**, *72*, 508.
(24) Rhim, W. K.; Elleman, D. D.; Vaughan, R. W. *J. Chem. Phys*. **1973**, *58*, 1772–1773.
(25) VanderHart, D. L.; Barnes, J. D.; St. John Manley, R. *Macromolecules* **1994**, *27*, 2826.
(26) Sirringhaus, H.; Brown, P. J.; Friend, R. H.; Nielsen, M. M.; Bechgaard, K.; Langeveld-Voss, B. M. W.; Spiering, A. J. H.; Janssen, R. A. J.; Meijer, E. W.; Herwig, P.; de Leeuw, D. M. *Nature* **1999**, *14*, 685–688.

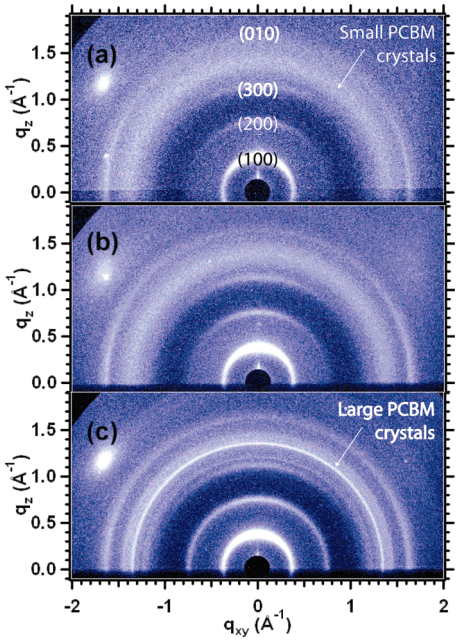

Figure 2. Grazing-incidence X-ray diffraction patterns of the P3HT/PCBM blend after (a) no annealing, (b) 100 °C annealing, (c) 150 °C annealing. P3HT peaks are indexed; PCBM contributes a diffuse ring (a,b) that sharpens after 150 °C annealing (c), indicating increased crystal size or order. The radially averaged patterns are given in the Supporting Information (Figure S2); q2 = qxy2 + qz2. The standard uncertainty of q is 1% and is determined by the accuracy of calibration of the sample to detector distance.

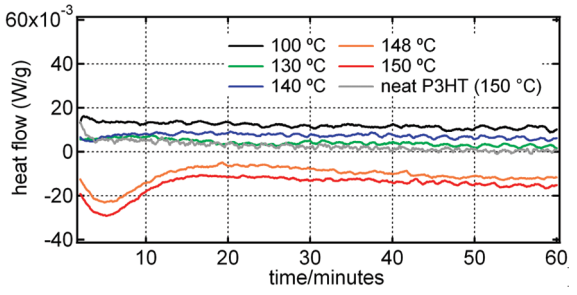

Figure 3. Isotherms of P3HT/PCBM at temperatures from 100 to 150 °C. An isotherm for pure P3HT cast from chlorobenzene is shown for comparison (gray curve). Exotherms are pointed down in the thermograms, and curves have been shifted vertically for optimal comparison. [The uncertainty in determining whether an exothermic process was occurring over the measurement time was estimated by comparison with measurements on an empty sample pan over a equivalent time frame. The noise levels (oscillations in heat flow over times of 1 min or less, ≈ 1 mW/g) and the drift in heat flow (change in magnitude of heat flow with time, ≈0.8 $\mu W \cdot g^{-1} s^{-1}$) for the blend samples measured at temperatures below 148 °C were indistinguishable from those of the empty pan.].

evidence of larger and/or more ordered PCBM crystals. Increased PCBM crystal size would be accompanied by a greater extent of P3HT/PCBM phase separation.

Differential Scanning Calorimetry. This crystallization behavior is further evidenced in differential scanning calorimetry (DSC) isothermal measurements shown in Figure 3. No exothermic process indicative of crystallization is observed on the time scale of minutes at temperatures as high as 140 °C, but exotherms are observed at 148 °C and higher. These exotherms coincide with an increase in PCBM crystallinity by GIXD, and occur when the temperature exceeds the glass transition temperature

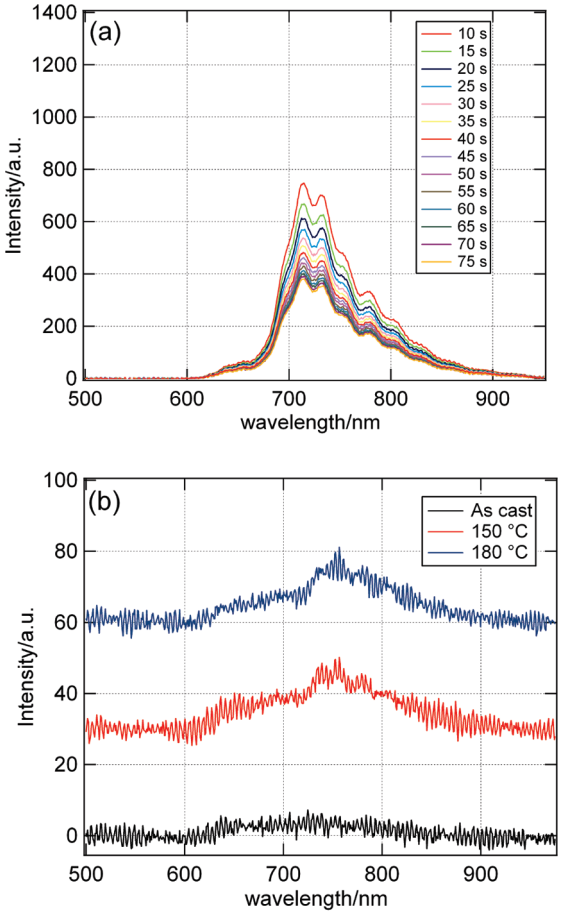

Figure 4. (a) PL spectra of P3HT for the indicated total irradiation times. (b) PL spectra for the P3HT/PCBM as-cast blend, 150 °C-annealed blend, and 180 °C annealed blend.

of PCBM (≈140 °C).[27] For comparison, a pure P3HT sample prepared identically to the blend (Figure 3, gray trace) showed no visible exothermic process at 150 °C.

PL Measurements. To confirm the intimacy of mixing in the bulk blends of P3HT/PCBM, PL quenching measurements were taken (λ = 442 nm); the spectra are given in Figure 4. As shown in Figure 4a, neat P3HT had a very intense PL signal from 650 to 850 nm that photobleached in tens of seconds. To estimate the full P3HT PL signal, the integrated spectrum was plotted versus total irradiation time, and fit to the function $I_0 \exp(-t/t_{decay})$ (data not shown). The I_0 parameter was taken to be the estimate of the neat P3HT signal.

The PL signal of the as-cast blend, shown in Figure 4b, was severely quenched to less than 0.5% of the neat P3HT PL signal intensity, whereas the annealed blend (150 °C for 1 h), shown in Figure 4b, recovered slightly to a value of 5% of the neat P3HT signal. Very aggressive annealing (180 °C for 20 h) resulted in no further increase of PL signal. All blends were photostable on the time scale of the experiment (1 to 2 min) regardless of heat treatment.

^{1}H Solid-State NMR. CRAMPS spectra are given in Figure 5 of the blend (5a), neat P3HT (5b) and neat PCBM (5c). As seen in Figure 5b, the P3HT protons are

(27) Zhao, J.; Swinnen, A.; Assche, G. V.; Manca, J.; Vanderzande, D.; Mele, B. V. *J. Phys. Chem. B* **2009**, *113*, 1587–1591.

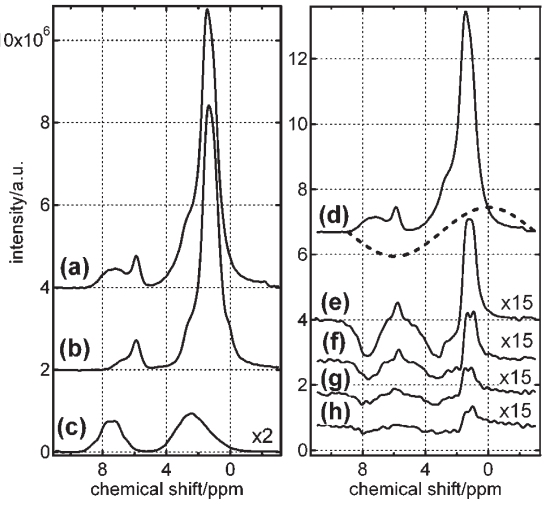

Figure 5. (a–c). Stack plot of ^{1}H CRAMPS spectra: (a) P3HT/PCBM blend, (b) P3HT, (c) PCBM. (d–h) Stackplot of chemical-shift-based spin diffusion NMR spectra of the P3HT/PCBM blend for various mixing times: (d) M_0 (repeat of (a), given as guide to the eye), (e) 2 ms, (f) 60 ms, (g) 180 ms, (h) 550 ms. The dashed line is an approximate excitation profile of the MREV-8 preparation.

almost all aliphatic (0 ppm to 3.8 ppm) with only a single aromatic thiophene proton (≈ 6 ppm). The thiophene resonance comprises a narrow component (5.8 ppm) and slightly downfield shoulder (6.5 ppm to 7.6 ppm), which we believe to be due to crystalline and glassy-amorphous domains, respectively. The spectrum of PCBM, on the other hand, is more strongly aromatic with five out of the fourteen total protons on the PCBM molecule belonging to the phenyl ring (6 ppm to 9 ppm). Intensity contributions to the blend spectrum are heavily weighted toward P3HT because PCBM is relatively proton dilute. The PCBM aromatic resonances appear in the blend spectrum as a mere shoulder on the single thiophene resonance of P3HT.

Although there is significant spectral overlap of the two components, the contrast in lineshapes is sufficient to conduct chemical-shift-based ^{1}H spin diffusion NMR experiments.[28] The MREV8 preparation step irradiation has been previously shown[10,11] to have the effect of multiplying the CRAMPS spectrum by a sine wave, the period of which is controlled by the total preparation time (MREV8 cycle time is 39.6 us and ten total cycles), and the phase of which is controlled by the offset frequency which was varied to be close to the zero-integral condition. The sinusoidal magnetization profile for these experiments is represented pictorially in Figure 5d demonstrating that a fixed magnetization gradient was established such that PCBM initially had negative magnetization, P3HT positive. The magnitude of this magnetization was measured as a function of mixing time (t_m); spectra for mixing times of 2 ms, 60 ms, 180 ms, and 550 ms are given in Figure 5e–h.

Spin Diffusion Plot. The resultant data were analyzed in a normalized spin diffusion plot[29] where one defines a

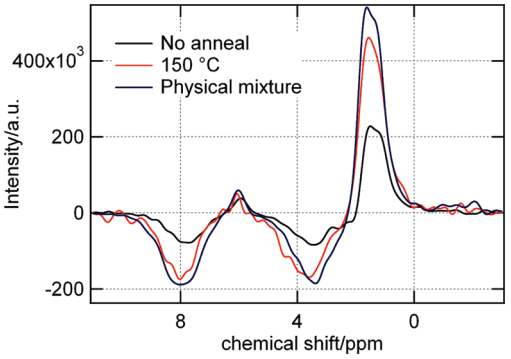

Figure 6. Stack plot of ^{1}H spin diffusion NMR spectra of the P3HT/PCBM blend (red and black lines) and physical mixture (blue line) for a mixing time of 2 ms.

quantity, ΔM, as a change of magnetization for either blend component. ΔM is scaled so that a completely coarsened, incompatible blend (no intercomponent spin diffusion) has an asymptote of unity, whereas sample-wide spin equilibration has an asymptote of zero (e.g., an intimately mixed blend). In such a normalized spin diffusion plot, the ordinate, ΔM, is plotted versus the square root of the mixing time, $t_m^{1/2}$. Decreases in intensity of the observed spin diffusion spectra will arise from three separate relaxation processes: intramolecular spin exchange, intercomponent spin exchange, and spin–lattice relaxation. Therefore, measures must be taken to isolate the intercomponent spin exchange since this process informs us about component mixing.

Intramolecular spin equilibration in both P3HT and PCBM occurs quite rapidly (1 to 2 ms) because of the physical proximity of all protons in both components. Intramolecular spin exchange, therefore, does not contribute to intensity changes for $t_m > 2$ ms. Furthermore, intensity changes that are due to intercomponent spin exchange for $t_m < 2$ ms are easily found by performing an identical experiment on the physical mixture at the same stoichiometry as the blend (or on the individual neat components followed by spectral deconvolution). The intensities of the blend spectra are then compared to the physical mixture spectra; all decreases in intensity are attributed to intercomponent spin exchange. The results are demonstrated in Figure 6, which is a stack plot of spectra of the 50/50 blend of P3HT/PCBM and the physical mixture (at the same stoichiometry) for a mixing time of 2 ms. As shown in the figure, the blend spectra are less intense than the physical mixture spectrum because intercomponent spin exchange occurs in the blend samples to varying degrees ($M_{\text{unanneal}} < M_{150\ ^\circ\text{C}}$). ΔM, therefore, can be considered the scaled physical mixture value. We note that the apparent chemical shifts in these spectra vary slightly from sample to sample since the chemical shift scale and the scaling factor (approximately 0.49) are slightly dependent on probe tuning and rf amplitude.

The effect of spin–lattice relaxation generally becomes pronounced at longer mixing times ($t_m > 75$ ms in our case) where t_m is a non-negligible fraction of T_1. These effects are usually accounted for on the spin diffusion plot by using a

(28) Caravatti, P.; Neuenschwander, P.; Ernst, R. R. *Macromolecules* **1985**, *18*, 1663.
(29) VanderHart, D. L.; McFadden, G. B. *Solid State Nucl. Magn. Reson.* **1996**, *7*, 45–66.

Table 1. Spin−Lattice Relaxation Times of P3HT and PCBM and Blends for Different Anneal Schedules [a]

composition	anneal T/°C	anneal time	T_1^{PCBM}/ms	T_1^{P3HT}/ms
P3HT	none			570
PCBM	none		narrow: 2600[b] broad: 4500	
50P3HT·50PCBM	none		760	660
50P3HT·50PCBM	150	60	1150	605
50P3HT·50PCBM	180	1200	1450 (or 500 and 2200)	590

[a] The T_1's of the blends were measured by deconvolution into the neat spectra and subsequent fitting to the equation $y = 1 - 2e^{-t/T_1}$. [b] Both a narrow component (4 kHz fwhm) and a broad component (40 kHz fwhm) of the Bloch decay spectrum was observed. This peak persisted even after annealing at temperatures (160 °C) slightly above the glass transition temperature of PCBM (≈ 140 °C) for multiple hours. [c] Fitting the PCBM magnetization to a single exponential led to very poor results and a biexponential fit was significantly better.

corrective multiplication factor, $\exp(+t_m/T_1)$, at each mixing time, t_m. Typically in blends that are mixed on size scales smaller than ≈50 nm, a single T_1 is exhibited, and applying this correction factor is straightforward.[30] In the case of our blend samples, however, a variety of domain sizes is observed (see Discussion below); the heterogeneity results in multiple T_1's (Table 1). This dispersion results in a loss of precision of the appropriate correction factor for the blend spin diffusion curve. In some cases, however, the correction factor can be exact, (e.g., for the physical blend employing a zero-integral analysis) and is given by

$$\frac{1}{\{\exp(-t_m/T_1^{PCBM}) + f_{PCBM}^{H} \cdot [\exp(-t_m/T_1^{PCBM}) - \exp(-t_m/T_1^{P3HT})]\}} \quad (1)$$

where f_{PCBM}^{H} is the proton fraction of PCBM, T_1^{P3HT} is the longitudinal relaxation time of P3HT, and T_1^{PCBM} is the longitudinal relaxation time of PCBM. A derivation of this correction factor is given in the Supporting Information.

The resultant normalized spin diffusion plot, properly corrected for longitudinal relaxation, has historically[9−14] been used to interpret the degree of phase separation in two-component blends in terms of stoichiometries, morphologies, and domain sizes. At early times, spin diffusion plots generally decay linearly and can be modeled with Fick's second law for an estimate of the domain size, x, using the equation[31]

$$x = \frac{\varepsilon}{f_d}\sqrt{\frac{4Dt_{1/2}^{*}}{\pi}} \quad (2)$$

where ε describes the dimensionality of the system (1 for lamellae, 2 for rods in a matrix, and 3 for spheres in a matrix), f_d is the volume fraction of the dispersed phase

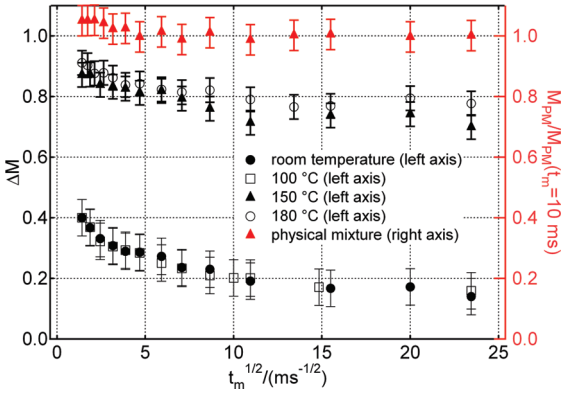

Figure 7. Spin diffusion plots of the 50/50 blend of P3HT/PCBM for various thermal schedules (black), and the 50/50 physical mixture of P3HT/PCBM (red). The blend data is a plot of ΔM vs $t_m^{1/2}$, whereas the physical mixture data is a plot of $M(t_m^{1/2})/M(t_m^{1/2} = (10)^{1/2}\ m\ s^{1/2})$. Error bars represent one standard deviation of expected uncertainty.

(in our case, 0.5), D is the spin diffusion coefficient (0.1 nm^2/ms to 0.8 nm^2/ms, typically),[32] and $t_{1/2}^{*}$ is the x-intercept of the linear fit (or the intercept of the asymptote if one exists). The asymptote of the spin diffusion plot is used as an estimate of the degree of phase separation to distances greater than approximately 100 nm.[33]

Discussion

Spin diffusion plots of the 50/50 blend of P3HT/PCBM for different anneal temperatures are shown in Figure 7. The unannealed and 100 °C annealed samples exhibit essentially identical spin diffusion behavior. This result indicates that no morphological changes occur at this annealing temperature, consistent with GIXD and DSC data. Both spin diffusion curves are marked with an initial fast decay to approximately $\Delta M = 0.4$, followed by a slower decay, which slowly approaches an asymptote of approximately 0.15. Assuming that the ^{1}H spin diffusion process is well-behaved, these curves suggest that a broad distribution of domain sizes exist in these bulk samples.

To illuminate the presence of a dispersion of sizes, numerical simulations were carried out for different domain sizes in both lamellar and rod/matrix morphologies.[34] The results are shown in Figure 8. As seen by comparison of the simulations to the experimental data, these data do not follow a single curve, but rather comprise a superposition

(30) We note for completeness that assignment of a "T_1" assumes exponential spin−lattice relaxation behavior, which may not be the case, particularly when significant spin exchange occurs. However, least-squares fits to exponentials were quite good ($R^2 > 0.99$), so T_1's were used for subsequent analysis.

(31) Schmidt-Rohr, K.; Spiess, H. W. *Multidimensional Solid State NMR and Polymers*; Academic Press: London, 1994.

(32) A generally accepted formula for the spin diffusion coefficient is $D = a\langle r^2\rangle\Delta\nu_{1/2}$, where $\langle r^2\rangle$ is the average square of the ^{1}H-^{1}H internuclear distance of closest approach, $\Delta\nu_{1/2}$ is the full-width at half-maximum of the Bloch decay spectrum, and a is a scaling factor (generally presumed to be 0.33). In the case of P3HT, $\langle r^2\rangle$ = 0.05 nm^2, $\Delta\nu_{1/2}$ = 16 kHz, which yields 0.3 nm^2/ms. The spin diffusivity of PCBM is probably much more complicated because of the inhomogeneous spatial proton distribution that results from the large intermolecular spacings (0.8 to 1.0 nm, see refs 35, 36). As a result, the anticipated intermolecular ^{1}H-^{1}H couplings (≈ 200 Hz) are significantly weaker than the intramolecular couplings (40 kHz full-width at half-maximum in the Bloch decay spectrum). We estimate D_{PCBM} = 0.05 nm^2/ms for our simulations (see Discussion), but acknowledge that this value is uncertain.

(33) The size scale of phase separation (100 nm) is a lower bound in the case of the potentially low ^{1}H spin diffusivity of PCBM (0.05 nm^2/ms). We note that if the ^{1}H spin diffusivity is much greater (say, 0.2 nm^2/ms to 0.4 nm^2/ms), then 200 nm is a more appropriate value.

(34) A morphology of spheres in a matrix ($\varepsilon = 3$) is not likely at this stoichiometry and was, therefore, not included.

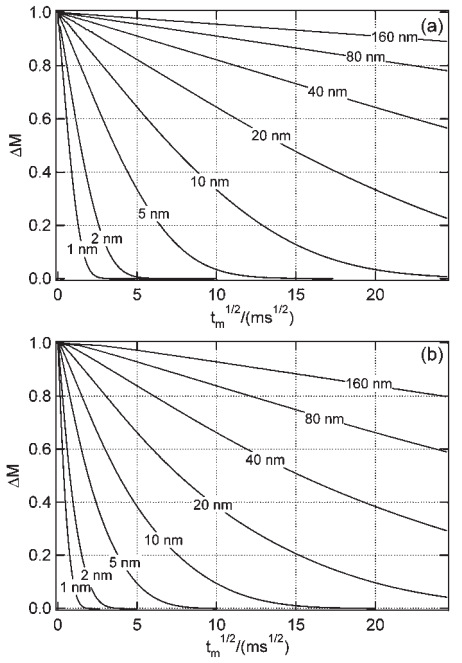

Figure 8. Simulated spin diffusion plots of the 50/50 blend of P3HT/PCBM for different domain sizes assuming both lamellar (a) and rod-in-matrix (b) morphologies. The spin diffusion coefficients of P3HT and PCBM were assumed to be 0.3 nm^2/ms and 0.05 nm^2/ms, respectively. The domain sizes indicated on the plot are for (a) a single lamellar thickness and (b) the rod diameter. The simulations were performed assuming 50/50 by volume.

of several curves. The initial fast decay is indicative of some PCBM being almost molecularly dispersed in a P3HT matrix (1 to 5 nm domains), whereas the region of slower decay suggests the presence of slightly larger domains of PCBM (tens of nanometers). The asymptote is consistent with long-range (> 100 nm) compositional heterogeneities, which is supported by our finding of slightly different longitudinal relaxation times for the two components. In our spin diffusion simulations, we have assumed a low spin diffusion coefficient for the PCBM domains (0.05 nm^2/ms) since the intermolecular $^1H-^1H$ couplings are anticipated to be weak ($\approx$ 200 Hz).[35] The spin diffusion coefficient of P3HT was calculated to be 0.3 nm^2/ms. We note though that although we do not know the absolute spin diffusion coefficients of P3HT and PCBM outright, their exact values do not alter our conclusions because they would affect the slopes only slightly (note that $x \propto (D)^{1/2}$).

The 150 °C annealed sample exhibits a spin diffusion curve that is significantly different than those for the as-cast and 100 °C annealed sample. The fast decay component remains present after this higher anneal, but represents a smaller portion of the spin diffusion curve, indicating that the amount of PCBM in very small domains (1 to 5 nm) is dramatically reduced. An intermediate decay is still observed, albeit slightly diminished. Importantly, a new asymptote is observed at $\Delta M = 0.7$. This asymptote is clear evidence of phase separation to distances greater than $\approx$100 nm, which indicates the growth of larger PCBM crystals. Furthermore, the $\Delta M = 0.7$ asymptote supports our finding that the T_1's of the components become more disparate (Table 1) since a greater number of P3HT and PCBM proton spins are out of spin diffusion contact with one another (and, hence, do not share a T_1).

Although the spin diffusion results do not uniquely describe the compositions of phases within the blend, they do place quantitative constraints on possible distributions. Complete phase separation of both components into large pure phases is not a possible interpretation because ΔM shows significant decay regardless of heat treatment. This conclusion is supported by the persistence of PL quenching (Figure 4), even after annealing at 180 °C. For example, if PCBM forms large, pure domains, the 150 °C-annealed data suggest that only 74% could do so; the remaining 26% must remain in a P3HT-rich phase of composition (by mass) 0.79 P3HT·0.11 PCBM. Alternatively, if P3HT forms large, pure domains (which is not likely because of persistent PL quenching), then 94% of it could do so with the remaining 6% in a PCBM-rich phase of composition 0.06 P3HT·0.94 PCBM. These two scenarios represent limiting constraints; all intermediate scenarios consistent with an asymptote of 0.7 can be found via the equation in the Supporting Information.

The authors further note that a three-phase system (neat-P3HT, neat-PCBM, mixed phase) could also explain the asymptote of the spin diffusion curve of the 150 °C annealed blend (Figure 7, black triangles). An example three-phase system would be sparsely distributed PCBM molecules kinetically trapped in a P3HT-rich phase. This scenario would represent a blend that is incompletely phase separated, which, if annealed for longer times, would presumably phase separate into pure phases. We tested this possibility by using more aggressive annealing conditions (180 °C for 20 h), and found there to be no net change in PL signal intensity (blue line, Figure 4b). Furthermore, both the 150 and 180 °C annealed samples exhibit nearly identical spin diffusion behavior within the uncertainty of our experiment (Figure 7). This suggests that no further phase separation occurs after 1 h when annealing at 150 °C, and that the three-phase system is not a likely scenario.

We posit that ^1H spin diffusion NMR is a technique that can be generally applied to quantify the domain size distribution and phase behavior in all conjugated-polymer/PCBM-based BHJs, even in samples that exhibit a broad dispersion of domain sizes, where other analytical techniques may fail. We caution that conclusions drawn from such data hinge upon the assumption that the spin diffusivity of the protons in the PCBM domains is "well-behaved" (isotropic, morphologically independent, and Fickian in nature). Despite the fact that the protons in neat PCBM seem rather rigid (full width at half-maximum of 40 kHz in the Bloch decay spectrum), the spatially inhomogeneous distribution could result in non-ideal behavior, particularly in morphologies which exhibit very heterogeneous networks of protons. An example is the layered morphology recently found in the

(35) The couplings were calculated from the dipolar interaction equation. For a thorough description of dipolar couplings, see Abragam, A. *Principles of Nuclear Magnetism*; Clarendon Press: Oxford, 1961.

PCBM/*o*-dichlorobenzene co-crystal.[36] It has recently been shown that PCBM crystal structure is strongly dependent on solvent choice,[37] so correlation of morphology to spin diffusivity may be important for comparing blends of different preparation recipes. Work is underway to understand these effects, and, in turn, to improve the precision of quantities extracted from the spin diffusion curve.

Conclusions

These results demonstrate that ^{1}H solid-state NMR is a powerful means to measure the structure of BHJ blends. Truly nanoscale domain sizes can be estimated, and explicit compositional constraints can be placed on the distribution of phases. Very small PCBM domains persist even in the presence of larger crystals that grow because of a thermal annealing process. Even aggressive annealing is not sufficient to induce complete phase separation of either component in these samples. We are currently extending this work to thinner, more technologically relevant BHJ films for direct correlation to device properties. Extension to thin films requires special sample preparation;[38] in these sample-limited regimes, ^{1}H NMR has a clear advantage over other nuclei in that it is very sensitive and requires no isotopic labeling.

Acknowledgment. R.C.N. acknowledges support from the National Research Council postdoctoral fellowship program. Babak Nikoobakht is acknowledged for his assistance with the PL measurements. C. L. Soles and other members of the National Institute of Standards and Technology Electronics Materials Group are acknowledged for valuable discussions.

Supporting Information Available: The XRD data (Figure S1), and details regarding the spin diffusion plot. This material is available free of charge via the Internet at http://pubs.acs.org.

(36) Ripsens, M.; Meetsma, A.; Rittberger, R.; Brabec, C. J.; Sariciftci, N. S.; Hummelen, J. C. *Chem. Commun.* **2003**, 2116–2118.
(37) Yang, X.; van Duren, J. K. J.; Rispens, M. T.; Hummelen, J. C.; Janssen, R. A. J.; Michels, M. A. J.; Loos, J. *Adv. Mater.* **2004**, *16*, 802–806.
(38) VanderHart, D. L.; Prabhu, V. M.; Lavery, K.; Dennis, C. L.; Rao, A.; Lin, E. K. *J. Magn. Reson.* **2009**, *201*, 100–110.